**To cite this version :**

Elio Antonio BUFI, Paola CINNELLA, Xavier MERLE, Paola CINNELLA - Sensitivity of Supersonic ORC Turbine Injector Designs to Fluctuating Operating Conditions - In: ASME TURBO EXPO 2015, Canada, 2015 - Proceedings of the ASME 2015 Turbo Expo Turbine Technical Conference - 2015

# SENSITIVITY OF SUPERSONIC ORC TURBINE INJECTOR DESIGNS TO FLUCTUATING OPERATING CONDITIONS

**Elio A. Bufi**
Laboratoire DynFluid
Arts et Metiers ParisTech, Paris (France)
Politechnic of Bari, Bari (Italy)
Email: Elio-Antonio.BUFI@ensam.eu

**Paola Cinnella**[*]
Arts et Metiers ParisTech, Paris (France)
Email: paola.cinnella@ensam.eu
**Xavier Merle**
Laboratoire DynFluid
Arts et Metiers ParisTech, Paris (France)
Email: xavier.merle@ensam.eu

## ABSTRACT

*The design of an efficient organic rankine cycle (ORC) expander needs to take properly into account strong real gas effects that may occur in given ranges of operating conditions, which can also be highly variable. In this work, we first design ORC turbine geometries by means of a fast 2-D design procedure based on the method of characteristics (MOC) for supersonic nozzles characterized by strong real gas effects. Thanks to a geometric post-processing procedure, the resulting nozzle shape is then adapted to generate an axial ORC blade vane geometry. Subsequently, the impact of uncertain operating conditions on turbine design is investigated by coupling the MOC algorithm with a Probabilistic Collocation Method (PCM) algorithm. Besides, the injector geometry generated at nominal operating conditions is simulated by means of an in-house CFD solver. The code is coupled to the PCM algorithm and a performance sensitivity analysis, in terms of adiabatic efficiency and power output, to variations of the operating conditions is carried out.*

## NOMENCLATURE

$p$    Pressure.
$\rho$    Density.
$T$    Absolute temperature.
$R_g$    Specific gas constant.
$a$    Speed of sound.
$v_s$    Specific volume.
$\gamma$    Specific heat ratio.
$M$    Mach number.
$\varphi$    Flow angle evaluated between the velocity vector and the streamwise direction.
$\phi$    Leading edge angular extension.
$G$    Massflow rate.
$V$    Velocity magnitude.
$H_t$    Nozzle throat half-height.
$\Theta$    Blade vane stagger angle.
$R$    Radius for the design of the convergent.
$ch$    Axial chord.
$\beta_a$    Leading edge attach angle.
$\epsilon$    Blade thickness.
$\theta$    Stagger angle.
$H$    Specific enthalpy.
$S$    Specific entropy.
$\eta_{is}$    Isentropic efficiency.
$\beta$    Expansion pressure ratio.
$M_w$    Molecular weight.
$P$    Power output per unit of depth.
$n$    Total number of random parameters.
$N_p$    Order of the chaos polynomial.
$P_{PCM}$    Number of collocation points.
$\mu$    Mean.

$\sigma^2$  Variance.
   **Subscripts:**
$r$  Reduced: normalised respect to critical conditions.
$c$  Critical thermodynamic property.
$0$  Total/reservoir thermodynamic property.


## INTRODUCTION

   The use of dense gases as working media in turbomachinery, referred to as Organic Rankine Cycle (ORC) turbines, is proposed as a method of recovery of variable energy sources such as waste heat from industrial processes. Whereas a traditional Rankine Cycle operates with steam as the working fluid, ORC turbines use an organic fluid such as hydrocarbons, silicon oils or other organic refrigerants. The low critical temperature, high density and elevated heat capacities of these fluids result in high suitability for low temperature operation, even as low as $80^o$C [1]. Furthermore, the slope of the saturated vapor line for organic fluids eliminates the risk of condensate at the turbine outlet, without heating the working fluid into the superheated vapor region. ORCs represent a promising technology for the development of widely distributed, small yield (from 5 kW to 1 MW) thermal energy conversion devices [2]. Proposed heat sources for ORC turbines typically include variable energy sources such as solar thermal collectors or waste heat from industrial processes. As a result, to improve the feasibility of this technology, the resistance to variable input conditions must be taken into account at an early stage of the development process. In this way, it is possible to overcome the limitation of deterministic calculations that neglects the effect of uncertainties in design variables and/or design parameters. The sensitivity of the design with respect to variations of the design parameters, like geometrical tolerances or fluctuations of the operating conditions can be measured through the statistics such as mean and variance (or standard deviation) of a response. Hereafter, *statistics* will always designate mean and variance (see e.g. [3, 4]). In order to assess the influence of variability of operating conditions, thermodynamic and geometrical parameters on the performances of a ORC epxander, firstly an accurate deterministic design methodology for ORC expanders has been developed and tested. The methodology, taking properly into account dense gas effects, is based on a generalized method of characteristics (MOC). The MOC is well known as a powerful tool to solve hyperbolic partial differential equation systems and, in inverse design, can be advantageously used to design the nozzle divergent shapes [5–7]. This problem has been widely faced in classical gasdynamics, however only in recent years it has gained interest for real gas problems due to the great improvements in the dense gases thermodynamic modelling.

In this work the MOC algorithm allows to design supersonic nozzles under dense gas effects. Besides, a geometrical post-processing is applied in order to design the ORC axial injector vane shape. This methodology is coupled with an algorithm for the uncertainty quantification applied to the computational fluid dynamics, that implements the Probabilistic Collocation Method (PCM). The purpose is to evaluate the sensitiveness of the performances of ORC expanders designed with the new methodology to stochastic variations of the design parameters.
Secondly, the injector performances at nominal point are evaluated by means of an in-house CFD solver equipped with a set of equations of state (EOS), suitable for real gas calculations. Finally, an uncertainty quantification analysis is carried out by coupling the numerical solver with the PCM algorithm and evaluating the sensitivity of injector performances to variability of operational, geometrical and thermodynamic parameters.


## DENSE GAS DYNAMICS

   Dense gases are defined as single phase vapors in thermodynamic conditions close to saturation curves, characterized by complex molecules and moderate to large molecular weights.
When the thermodynamic conditions are such that pressure and density are sufficiently low, any gaseous substance can be considered in the dilute gas region and described with the well known equation of state of perfect gases:

$$p = \rho R T \qquad (1)$$

However, in many practical turbomachinery applications, such as ORC systems, the working fluid thermodynamic conditions are close to the critical point and the real gas effects, due to strongly non-linear molecular interactions, are no more negligible. In this case Eqn. (1) is modified by introducing a compressibility factor $Z = p/\rho RT$, which is always below 1 for real gases and measures the deviation from the ideal gas behaviour, for which $Z = 1$. For pure substances, $Z$ can be calculated as a function of the reduced thermodynamic properties (i.e. normalized with respect to critical point properties), according to the *law of corresponding states*. Such calculations are based on simple molecular dynamics models [8]. For more complex molecules, simple EOS are no longer accurate and the use of more complex multi-parameter EOS is required. Examples of such multi-parameter EOS are given later.
The dynamics of dense gases can be described through a key thermodynamic property, known as the Fundamental

Derivative [9]:

$$\Gamma = \frac{a^4}{2v^3}\left(\frac{\partial^2 v}{\partial p^2}\right)_s = 1 + \frac{\rho}{a}\left(\frac{\partial a}{\partial \rho}\right)_s \qquad (2)$$

The study of Eqn. (2) provides informations about the behaviour of thermodynamic properties and represents a measure of the rate of change for the local speed of sound. The value of $\Gamma$ and its sign are good revealers of local dense gas phenomena. In flow regions where $\Gamma > 1$, the gas shows a classical behaviour: the speed of sound drops in isentropic expansions, rises in isentropic compressions and only compression shock waves are allowed. So, by virtue of the Second Law of Thermodynamics, it can be shown [10] that only negative variations of the specific volume are possible across a shock. This is the case of perfect gases described by Eqn. (1), having a constant $\Gamma = (\gamma+1)/2$. If $0 < \Gamma < 1$, it is possible to observe a reverse behaviour with respect to the previous one, but still only compression shock waves are allowed although the related shock losses are lower.
Fluids characterized by a region of negative $\Gamma$ values in the vapor phase are called Bethe-Zel'dovich-Thompson (BZT) fluids and can show strongly non-linear behaviour close to the critical conditions and the saturation curves. When $\Gamma < 0$, compression shock waves are forbidden and only expansion shock waves are physically possible [11]. This phenomenon is theoretically predicted for a small amount of organic fluids (siloxanes, heavy hydrocarbons, heavy fluorocarbon such as PP10, PP11, PP25 etc.) in particular thermodynamic conditions and it will not be investigated here.
Another important feature of dense gases resides in the viscous behaviour, that is very different from the light gases one. Indeed, this is intermediate between that of liquids, for which viscosity tends to decrease with increasing temperature, and that of gases, with an opposite variation. The dynamic viscosity $\mu$ and the thermal conductivity $\kappa$ cannot be considered independent from temperature and pressure in the real gas regions. In a similar way, the approximation of a constant Prandtl number $Pr$ does not hold any more. Its behaviour tends to be controlled by variations of the isobaric specific heat $c_p$ , the thermal conductivity showing variations with temperature and pressure similar to viscosity. In the supercritical regime, where $c_p$ becomes large, strong variations of $Pr$ can be observed, in contrast with the behaviour of perfect gases. The viscous behaviour of dense gas flow has been discussed in [12].

**GOVERNING EQUATIONS**

We consider the conservation equations for single-phase, inviscid, non reacting flow, written in integral form for a control volume $\Omega$ with boundary $\partial\Omega$:

$$\frac{d}{dt}\int_\Omega \mathbf{w}\,d\Omega + \int_{\partial\Omega} \mathbf{f}\cdot\mathbf{n}\,dS = 0 \qquad (3)$$

In Eqn. (3), $\mathbf{w}$ is the conservative variable vector, where

$$\mathbf{w} = (\rho, \rho\mathbf{v}, \rho E)^{\mathbf{T}}$$

$\mathbf{n}$ is the outer normal to $\partial\Omega$, and $\mathbf{f}$ the flux density:

$$\mathbf{f} = \left(\rho\mathbf{v}, -p\overline{\overline{I}} + \rho\mathbf{v}\mathbf{v}, \rho\mathbf{v}H\right)^{\mathbf{T}}$$

where $\mathbf{v}$ is the velocity vector, $E$ the specific total energy, $H = E + p/\rho$ the specific total enthalpy, $p$ is the pressure, $\rho$ is the density and $\overline{\overline{I}}$ is the unit tensor. The preceding equation are completed by a thermal equation of state:

$$p = p(\rho(\mathbf{w}), T(\mathbf{w})) \qquad (4)$$

where $T$ is the absolute temperature, and by a caloric equation of state for the specific internal energy $e$. In this work the thermodynamic behaviour of ORC working fluids is described through the Peng-Robinson-Stryjek-Vera (PRSV) cubic EOS [13], which has been proven to represent a good compromise between accuracy and computational cost (see, e.g. [14]). In this case, the caloric behaviour is modelled by assuming that the isocoric specific heat in the dense gas limit follows a simple power law. The robustness of this equation with respect to more complex and potentially more accurate multi-parameter equations of state of the Span-Wagner type [15–17] has previously been discussed [14]. In the PRSV model, Eqn. (4) is replaced by:

$$p = \frac{R_g T}{v - b} - \frac{a}{v^2 + 2bv - b^2}. \qquad (5)$$

where $p$ and $v$ denote respectively the fluid pressure and its specific volume, $a$ and $b$ are substance specific parameters related to the fluid critical-point properties $p_c$ and $T_c$. To achieve high accuracy for saturation pressure estimates of pure fluids, the temperature-dependent parameter $a$ in

Eqn. (5) is expressed as:

$$a = \left(0.457235 R_g^2 T_c^2 / p_c^2\right) \cdot \alpha\left(T\right) \qquad (6)$$

while

$$b = 0.077796 R_g T_c / p_c \qquad (7)$$

These properties are not completely independent, since the EoS should satisfy the conditions of zero curvature and zero slope at the critical point. Such conditions allow computing the critical compressibility factor $Z_c = (p_c v_c)/(R T_c)$ as the solution of a cubic equation. Note that the correction factor $\alpha$ is given by:

$$\alpha\left(T_r\right) = \left[1 + K\left(1 - T_r^{0.5}\right)\right]^2 \qquad (8)$$

with

$$K = 0.378893 + 1.4897153\omega - 0.1713848\omega^2 + 0.0196554\omega^3 \qquad (9)$$

The parameter $\omega$ is the fluid acentric factor. The caloric behavior of the fluid is approximated through a power law for the isochoric specific heat in the ideal gas limit:

$$c_{v,\infty}\left(T\right) = c_{v,\infty}\left(T_c\right)\left(\frac{T}{T_c}\right)^n \qquad (10)$$

with $n$ a material-dependent parameter.

## DENSE GAS SOLVER

In the numerical simulations presented in this work, the governing equations are discretized using a cell-centered finite volume scheme for structured multi-block meshes of third-order accuracy, which allows the computation of flows governed by arbitrary EOS [18]. The scheme is obtained by correcting the dispersive error of the classical second-order-accurate Jameson's scheme [19]. To preserve the high accuracy on non-Cartesian grids, the numerical fluxes are constructed by using weighted discretization formulas, which take into account the mesh deformations [20]. This ensures to achieve third-order accuracy on moderately distorted meshes and second-order accuracy at least on highly deformed mesh. The equations are then integrated in time using a four-stage Runge-Kutta scheme. Local time stepping, implicit residual smoothing and multi-grid accelera-

tion are used in order to drive the solution to the steady state. The accuracy of the numerical solver has been already demonstrated in previous works [18, 21].

## METHOD OF CHARACTERISTICS FOR DENSE GASES

In order to achieve a fast preliminary design of supersonic turbine nozzles we develop a design tool based on the MOC. The resulting geometry can be further improved using shape optimization method, however this is beyond the scope of this paper.

The MOC for dense gases is developed under the hypotheses of 2D, homentropic, steady flow. By stating the initial value problem, the conservation laws can be written as follow [6]:

$$\frac{dy}{dx} = \pm\frac{1}{\sqrt{M^2 - 1}} \qquad (11)$$

$$d\varphi \pm \sqrt{M^2 - 1}\frac{dV}{V} = 0 \qquad (12)$$

where the sign "$+$" denotes a left-running and "$-$" a right-running characteristic line; the coordinates $(x, y)$ are evaluated on a generic characteristic curve. Eqn. (11) represent the local slope of the characteristics; Eqn. (12) are compatibility relations stating conservation of momentum along the characteristics. Equations (11)-(12) are obtained without hypotheses on the EOS and can be solved simultaneously with the numerical procedure described in the following.

First of all, the MOC is initialized by the definition of the following design parameters: upstream total (reservoir) conditions $(p_0, T_0)$; target pressure distribution along the nozzle axis $p(x)$; design massflow rate $G$.

The calculation of the throat region, where the flow is transonic, is carried out by implementing Carriere's method [22], adapted to real gases. In this way, the first characteristic curve is calculated.

Multi-parameter EOS based on Helmholtz free energy are used for taking carefully into account the dense gas effects. For the organic fluid considered in this study, the reference multi-parameter EOS contained in the software NIST-REFPROP ver. 9.1 is used [23]. In the following, we refer to these equations by the acronym REF.

Equations (11)-(12) are numerically solved, based on a Heun predictor-corrector algorithm, of second order accuracy. By taking two consecutives points $(p-1), p$ on the same characteristic, the finite difference form of the compatibility

Eqn. (12) is:

$$\overline{A}(V_p - V_{p-1}) \pm (\varphi_p - \varphi_{p-1}) = 0 \qquad (13)$$

where $\overline{A}$ is the arithmetic average between points $(p-1)$ and $p$ of the quantity $A = \sqrt{M^2 - 1}/V$. Solving Eqn. (13), along with the Eqn. (12), results in an iterative procedure that provides the variables $(V, \varphi)$ and the coordinates $(x, y)$ of points lying on the considered characteristic line. The procedure described above is used to march along characteristic curves inside the nozzle and it is stopped when the massflow across the considered characteristic matches the design one. In this way the nozzle shape is determined.

Although the calculations required for the REF model are more complex than the ones required for other gas models, this algorithm remains very fast and only few seconds are required for obtaining results on a single-processor machine. When the chosen total conditions are such that the nozzle expansion goes through the multi-phase region of working fluid considered, the preceding algorithm fails to converge. When this happens, the nozzle design is simply restarted by choosing new total conditions for which no two-phase regions are formed.

## PROBABILISTIC COLLOCATION METHOD

The stochastic analysis used to determine the system response to input parameter variation is the non-intrusive Probabilistic Collocation Method (PCM) with a subsequent Lagrange interpolation, as developed by [24]. To illustrate the non-intrusive PCM implementation procedure, we consider the following uncertain differential equation system:

$$L(\mathbf{x}, \theta, \phi) = f(\mathbf{x}, \theta) \qquad (14)$$

Let us decompose the solution $\phi$ into deterministic: $\phi_i(\mathbf{x}, t)$, and stochastic: $h_i(\boldsymbol{\xi}(\theta))$, components:

$$\phi(\mathbf{x}, t, \boldsymbol{\xi}(\theta)) = \sum_{i=1}^{P_{PCM}} \phi_i(\mathbf{x}, t) h_i(\boldsymbol{\xi}(\theta)) \qquad (15)$$

where $\phi_i(\mathbf{x}, t)$ is the deterministic solution at the collocation point $\xi_s(\theta_i)$. In the PCM, $p$ is the order of the quadrature polynomial and the number of collocation points is given by $P_{PCM} = p^n$, where $n$ represents the total number of random input variables. The term $h_i$ is the Lagrange interpolated chaos polynomial of order $N_p = p - 1$ that passes through the $P_{PCM}$ collocation points:

$$h_i(\boldsymbol{\xi}(\theta)) = \prod_{s=1}^{n} \left[ \prod_{\substack{k=1 \\ k \neq i}}^{N_p} \frac{\xi_s(\theta) - \xi_s(\theta_k)}{\xi_s(\theta_i) - \xi_s(\theta_k)} \right] \qquad (16)$$

The collocation points are chosen as the roots of a quadrature polynomial of the same type of chaos polynomials adapted for the solution expansion. These in turn are selected according to the Askey scheme [25]. A decoupled deterministic CFD simulation is carried out at the $p$ collocation points for each uncertain parameter, permuted by a full factorial design, resulting in $P_{PCM} = p^n$ independent deterministic simulations. With all of the deterministic simulations completed, the output statistics can be calculated using a reconstructed Monte Carlo (RMC) method on the Lagrange interpolation. A large number ($N_{RMC} \approx 10000$) of values of $\xi_s(\theta)$ are selected from the uniform distribution of each input parameter and substituted into Eqn. (16). This equation rapidly reconstructs $h_i$, which is inserted into Eqn. (15). Finally, the statistical moments of each output parameter distribution can finally be calculated using the classical definitions on the sample generated by the RMC method.

## DETERMINISTIC RESULTS

An application of the MOC algorithm at nominal operating conditions is here proposed. The prescribed working fluid is the *1,1,1,3,3-pentafluoropropane*, well known as R245fa. This is a *dry* organic fluid suitable for ORC applications, non-toxic and with no ozone depletion potential. The nominal operating conditions are chosen very close to the critical point in order to involve dense gas effects in the design process. Here, the pressure distribution along the nozzle center-line is defined in order to match a pre-defined exit Mach number, $M_e$ (see Tab. 1). The massflow $G$ is defined per unit of length in the spanwise direction.

These operating conditions are representative of a typical small scale axial ORC action turbine ($\approx 25$ kW), where the entire enthalpy jump is elaborated in one single stage. As a consequence, the turbine is heavily loaded and strongly supersonic flow develops in the nozzle blade vanes.

The MOC allows to design the nozzle divergent. The design is completed by adding the convergent part, the shape of which is simply derived from geometrical considerations. Being the flow in the divergent supersonic, any geometry of subsonic nozzle convergent leads to the desired pressure ratio and massflow. The convergent is obtained as a concatenation of circular arcs whith a radius $R$ defined such

**TABLE 1**. NOMINAL OPERATING CONDITIONS FOR THE *MOC* ALGORITHM.

| $p_r^0$ | $T_r^0$ | $G$ [kg/s-m] | $M_e$ | Fluid |
|---------|---------|--------------|-------|--------|
| 0.98 | 1.13 | 20.0 | 2.06 | R245fa |

that $R/H_t > 6$ [6] (see Fig. 1). For this application, the MOC algorithm provides a nozzle throat-to-exit pressure ratio of 7.3 and a Mach number field described by the iso-contour lines in Fig. (8).

These results have been accurately verified by means of comparisons with results obtained for Euler calculation in the same geometric and operational conditions. The MOC results are shown to be in good agreement with the Euler ones, with slight differences but all below 1% (see Fig. 3-4).



**FIGURE 2**. MACH NUMBER CONTOUR PLOT OBTAINED WITH THE *MOC* ALGORITHM.



**FIGURE 1**. NOZZLE DESIGN WITH *MOC* ALGORITHM.
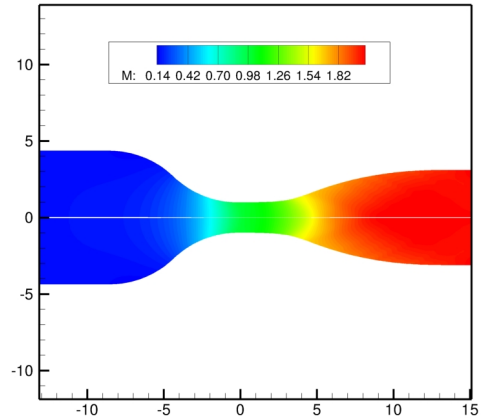


**FIGURE 3**. MACH NUMBER CONTOUR PLOT OBTAINED FOR THE *MOC*-BASE NOZZLE SHAPE GEOMETRY BY INVISCID CALCULATION. THE SUBSONIC PART IS ADDED WITH GEOMETRICAL POST-PROCESSING OF THE DIVERGENT GEOMETRY.

## Blade vane design and testing

Once that the complete nozzle geometry is obtained, a further geometrical post-process is applied in order to get the desired axial injector shape.

Knowing the main geometrical features of the turbine, such as the axial chord $ch$, the stagger angle $\theta$ and the blade pitch (c-c') (see Fig. 5), the blade vane is designed in the following way:

1. The suction side (d-e) is obtained by rotating the NODEC nozzle geometry by the angle $\theta$ in clockwise direction;

2. Given $ch$ and the coordinates of point (c), the leading edge (d-b) is designed as a circular arc with radius $R$;

3. An angle $\phi$ controls the angular extension of the pressure side part of leading edge (c-b), which has a radius $f \cdot R$, $f$ being a factor with value in the range [0.1; 1];

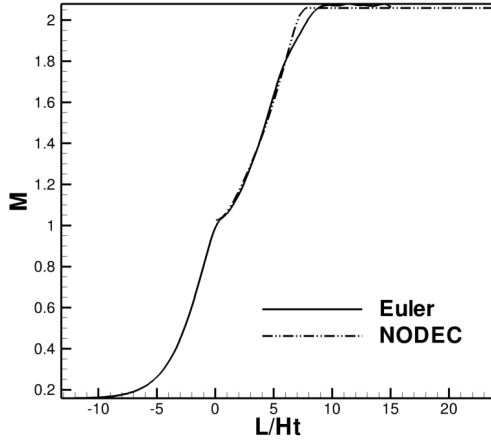4. The pressure side (b-a) is designed as a third order poly-

**FIGURE 4**. COMPARISON BETWEEN THE *MOC* (NODEC) AND THE INVISCID (EULER) MACH NUMBER EVOLUTIONS ALONG THE NOZZLE AXIS.

coordinates (a)-(b) and the angles $\phi$ and $\theta$;

5. The aft part (a-f) is determined by translating the upper part of nozzle profile by a distance equal to the pitch;

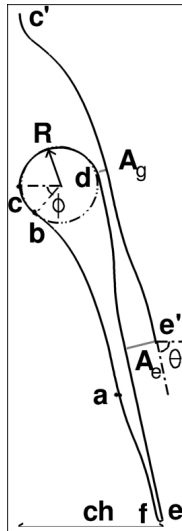6. A third order polynomial fits the points (f)-(e) and the value of $ch$ in order to obtain the trailing edge.



**FIGURE 5**. *ORC* TURBINE INJECTOR DESIGN: $A_g$, $A_e$ BEING THE NOZZLE THROAT AND EXIT SECTION, RESPECTIVELY.

**TABLE 2**. GEOMETRICAL PARAMETERS FOR THE INJECTOR DESIGN.

| $\theta$ | $R/H_t$ |
|----------|---------|
| 77.8°    | 7.5     |

The injector shape designed with the technique described above, has been tested in the numerical solver under the nominal operating conditions of Tab. 1. Further geometrical design parameters are provided in Tab. 2.
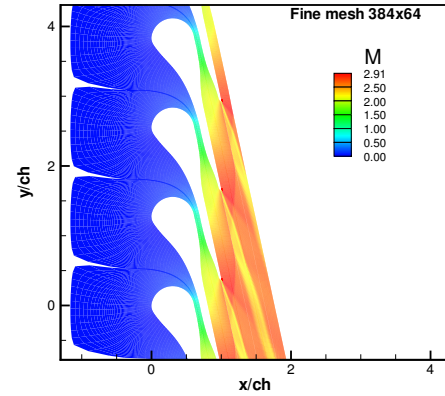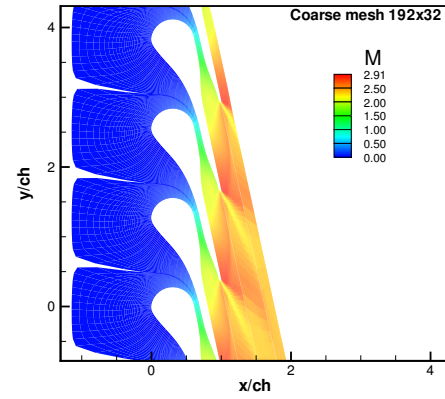


**FIGURE 6**. COMPARISON TEST BETWEEN MACH NUMBER CONTOUR PLOTS FOR A COARSE MESH (TOP) AND A REFINED MESH (BOTTOM).

Inviscid simulations have been carried out for the fine structured mesh. The inlet reduced total pressure and temperature, and a periodicity condition at inter-blade boundaries
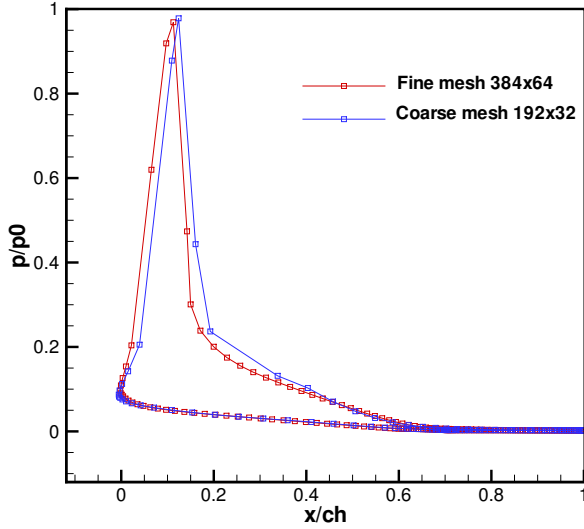
**FIGURE 7**. STATIC-TO-TOTAL PRESSURE RATIO ALONG THE BLADE WALL FOR AN INVISCID CALCULATION BOTH FOR COARSE (BLUE SQUARES) AND FINE (RED SQUARES) MESH.



**FIGURE 8**. MACH NUMBER CONTOUR PLOT.



**FIGURE 9**. STREAM-LINES AND MACH NUMBER CONTOUR PLOT.

are imposed. A no-match joint condition is applied to the branch-cut on the wake whereas an extrapolation condition is applied at the supersonic outlet. A slip condition involving a second order multi-domain extrapolation of the pressure from the inner cells is used. In order to assess numerical accuracy of the solutions further analysed, a preliminary mesh refinement study has been carried out. The inviscid results for a coarse structured mesh ($192 \times 32$ cells) in terms of Mach number and static-to-total pressure ratio profiles along the blade wall (see Fig. 6-7) have been compared with those obtain for a fine structured mesh ($384 \times 64$ cells). The two solutions show only slight differences in terms of pressure ratio estimated to be under 2%.

Then, numerical results on the finer grid are analysed in terms of both the overall characteristics of the flow fields generated through the machine (see Fig. 8) and the performance parameters of interest: isentropic efficiency $\eta_{is}$ (computed as the real-to-ideal static enthalpy drop ratio); power output per unit depth $P$. The flow is strongly supersonic and two weak oblique shock waves depart from the trailing edge: one impinges the suction side of the bottom blade, the other one interacts with the free stream downstream the vane. The flow accelerates up to Mach 2 in the nozzle exit section $A_e$, as predicted by the MOC design. Afterwards, the flow continues to expand guided by the suction side wall on the bottom and from a free stream surface on
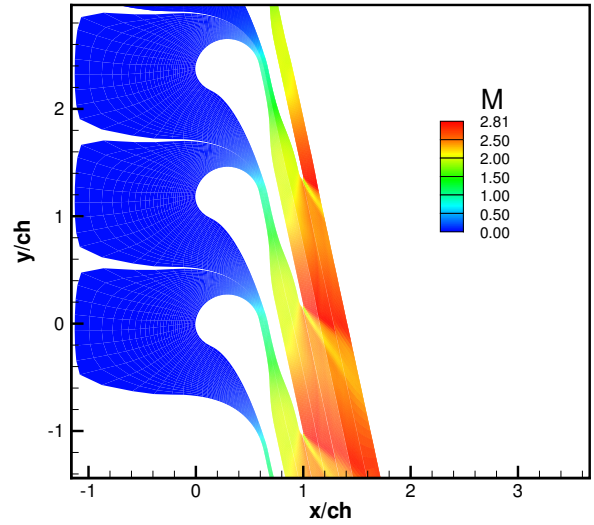
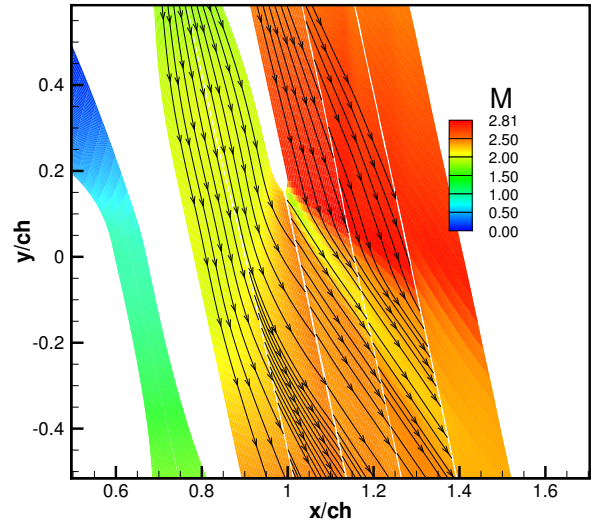the top. This effect leads the flow to Mach numbers higher than expected (up to $M \approx 2.7$). The flow is then weakly decelerated passing through the oblique shock. In addition to that, the shock induces an important deflection in the exit flow angle (see Fig. 9), which differs of about 60% from the geometrical one. This phenomenon needs to be taken
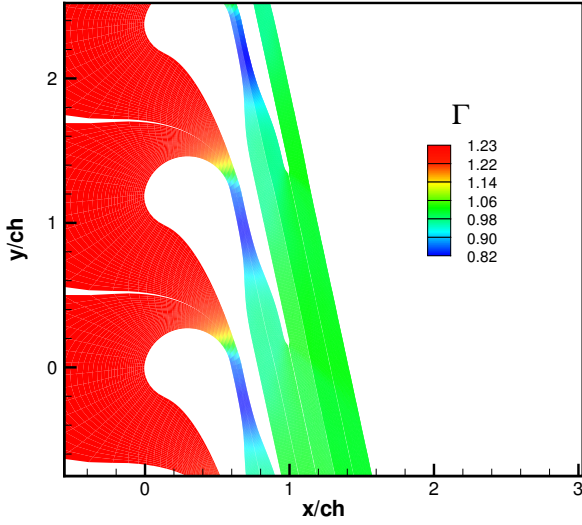
**FIGURE 10**. FUNDAMENTAL DERIVATIVE CONTOUR PLOT.

**TABLE 3**. INJECTOR PERFORMANCES.

| $\eta_{is}$ | $P[kW]$ |
|---|---|
| 0.947 | 196.27 |

carefully into account in the turbine stage design. The flow behaviour is also influenced by dense gas effects. As shown in Fig. 10, the flow starts to expand from thermodynamic conditions which are quite far from the saturation curves. This results in weak dense gas effects at the beginning, as confirmed by the fact that $\Gamma$ is greater than 1 in the subsonic part of the blade vane. During the expansion, the flow approaches the upper saturation curve and $\Gamma$ becomes lower than unity. As a consequence, the speed of sound increases during the expansion and the growth of the Mach number is slowed down. In the final part of the expansion $\Gamma$ increases again above unity and dense gas effects disappear.

Finally, the injector performances are provided in Tab. 3.

## STOCHASTIC RESULTS

In this section, the MOC algorithm previously described is coupled with the PCM algorithm in order to quantify the variability of the nozzle shape geometries and performances under variable operating conditions.

In the following we assume that all of the input random parameters, like the total pressure and temperature upstream

of the turbine, are independent. If some of the parameters were to be correlated, the method could be still applied by treating one of the parameters as random and by computing the other ones using the correlation law.

For the MOC application, the parameters with the greatest effect on the nozzle design are: the inlet total pressure $p_0$ and inlet total temperature $T_0$ (then, $n = 2$). As first approximation, a uniform continuous distribution is considered. Then, once defined the input parameters range variability $(a, b)$, the main statistics mean $\mu$ and variance $\sigma$ are calculated as follows:

$$\mu = \frac{a+b}{2} \tag{17}$$

$$\sigma^2 = \frac{(b-a)^2}{12} \tag{18}$$

A variation of $\pm 3\%$ of the reduced inlet total conditions around the nominal point $(p_r^0 = 0.98, T_r^0 = 1.13)$ is preliminarily considered. This choice allows to avoid the fall in the gas-liquid co-existence region of the state diagram during the gas expansion, which could implies issues from the numerical point of view. Indeed, for the ORC application here considered, the dense gas behaviour is studied by choosing nominal operating conditions as close as possible to the saturation curves (see Fig. 11) and their perturbations have to be accurately evaluated in order to avoid multi-phase expansions. By considering a second order Lagrange interpolated chaos polynomial, the total number of collocation points (and, then, of deterministic simulations) is $P_{PCM} = 9$.

The results are obtained again for the R245fa working fluid and they are firstly analysed from a geometrical sensitivity point of view. All the calculations are performed by keeping the target massflow constant and equal to 20 kg/s. The variability of the operating conditions induces a variability in the output nozzle design. In this case, the prescribed variation of operating condition results only in a slight modification of the nozzle geometry with respect to the one obtained at nominal operating conditions (see Fig. 13), with a maximum variation of only 0.01% of the exit-to-throat area ratio with respect to the mean value (nominal point). This shows that the MOC design is not strongly affected by the variability of the reservoir conditions when the mass-flow ratio is kept constant, which was expected for a perfect gas. For real gases, these variations lead essentially to modifications of the nozzle shape in the throat region.

Due to this considerations, we should expect that the sensitivity to variations of the main flow quantities, such as the
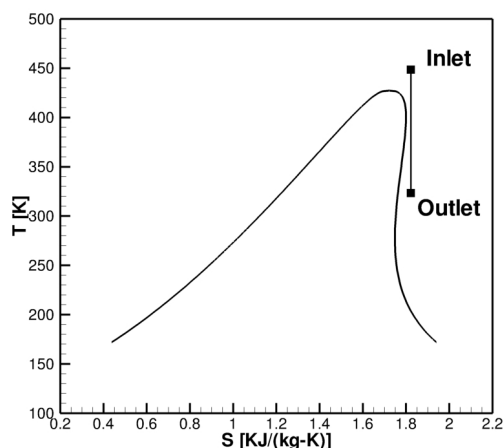
**FIGURE 11.** ISENTROPIC EXPANSION IN THE SUPERSONIC NOZZLE AT NOMINAL OPERATING CONDITIONS FOR *R245FA* FLUID.

Mach number, is very low. Indeed, inspection of top Fig. 12, displaying the percent coefficient of variation of the Mach number, the peak of variability of the solution, located close to the nozzle center-line, is of about 0.01%, which is negligible.

Bottom Fig. 12 shows the mean Mach number field applied to the mean nozzle shape and it is very similar to the one obtained for the nominal operating conditions.

In order to investigate the effect of large perturbations of the inputs conditions while avoiding to cross two-phase regions during the expansion, the Beta continuous distribution is selected because of its higher versatility. Indeed, by setting up its parameters to generate a non-symmetrical distribution, the Beta pdf can be advantageously used for increasing the inputs variability obtaining collocation points quite far from the saturation curves.

The four Beta parameters $\hat{\alpha}, \hat{\beta}, \bar{a}, \bar{b}$ (with $\hat{\alpha}, \hat{\beta}$ the pdf shape parameters and $\bar{a}, \bar{b}$ the lower and upper base interval limits) are estimated and fitted on the imposed input mean and variance. Now, a coefficient of variation of 8% respect to the nominal point $(p_r^0 = 0.98, T_r^0 = 1.13)$ is considered.

In Fig. 14 an increase of the geometric variability is shown. However, it remains still quite low with variations of the shape below 1%, even if the percent variation (see Fig. 15) is one order higher than before. This effect could be related to a substantial non-sensitivity of the MOC algorithm to input variations. Besides, the choice to impose a constant design massflow for all the calculations implies to keep the exit-to-throat nozzle area ratio constant. Then, the only
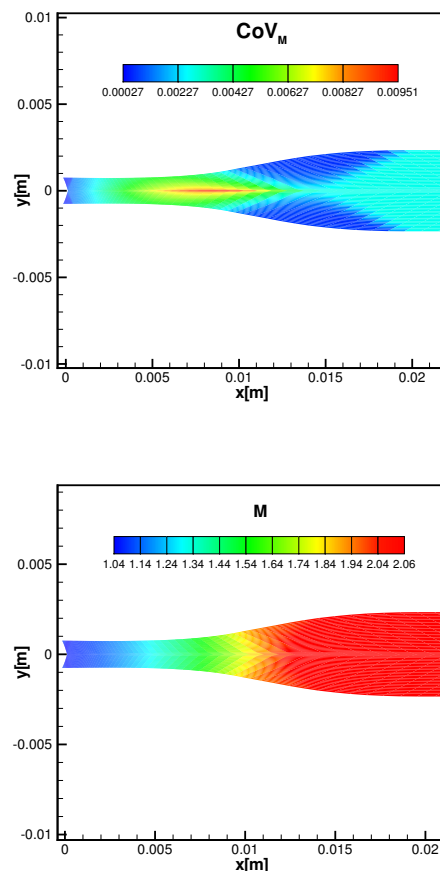


**FIGURE 12.** COEFFICIENT OF VARIATION (UPPER FIGURE) AND MEAN VALUE (LOWER FIGURE) OF THE MACH NUMBER FOR UNIFORMLY DISTRIBUTED INPUT PARAMETERS (±3% OF VARIATION AROUND THE NOMINAL POINT).

variations for real gas applications are due to the termodynamic model and to the variability of the specific heats ratio inside the nozzle. This results only in slight variations of the nozzle geometry in the accelerating part.

This analysis has been carried out also for the injector geometry, by coupling the inviscid dense gas solver with the PCM algorithm. In this case however, the inlet total conditions are varied with a fixed outlet pressure, leading to mass-flow variations. We then expect to observe a stronger impact of input uncertainties on the output solution. The results are shown in Fig. 16 and Fig. 17 under the form of percent coefficient of variation and mean Mach number, respectively. The mean flow field is similar to that obtained with the deterministic code described above and the same observations
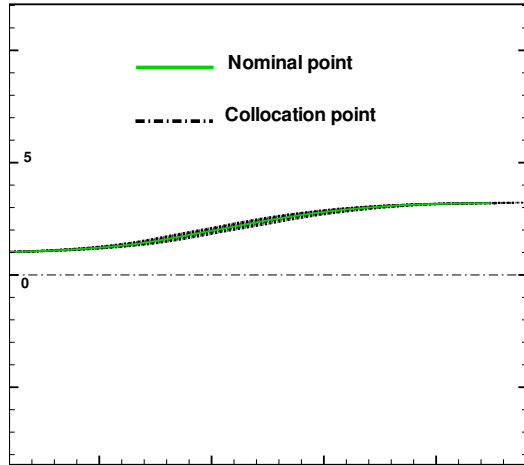
**FIGURE 13.** VARIABILITY OF THE NOZZLE SHAPE GE-OMETRY FOR UNIFORMLY DISTRIBUTED INPUT PA-RAMETERS (±3% OF VARIATION AROUND THE MEAN VALUE).
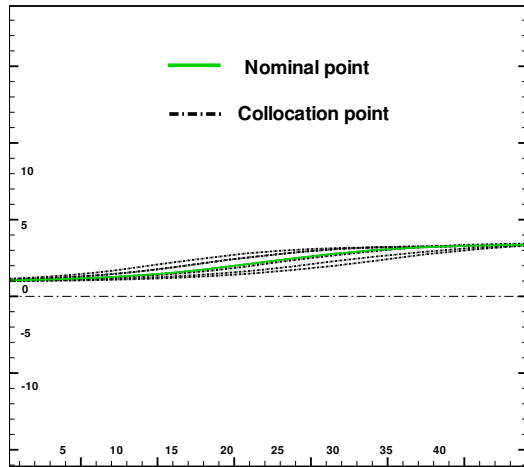


**FIGURE 14.** VARIABILITY OF THE NOZZLE SHAPE GE-OMETRY FOR BETA DISTRIBUTED INPUT PARAME-TERS (8% COEFFICIENT OF VARIATION).



**FIGURE 15.** COEFFICIENT OF VARIATION OF THE MACH NUMBER FOR BETA DISTRIBUTED INPUT PA-RAMETERS (8% COEFFICIENT OF VARIATION).



**FIGURE 16.** COEFFICIENT OF VARIATION OF MACH NUMBER FOR BETA DISTRIBUTED INPUT PARAME-TERS (8% COEFFICIENT OF VARIATION) FOR AN INVIS-CID STOCHASTIC CALCULATION.

can be addressed. Nevertheless, significant variability of the Mach number can be observed by analysing the coefficient of variation. Some zones of high uncertainty are located in correspondence of the oblique shocks and wake departing from the trailing edge, with contributions between 4% and 10%. The highest variability zone is located on the stagnation point at the blade leading edge, with a contribution of about 16%.
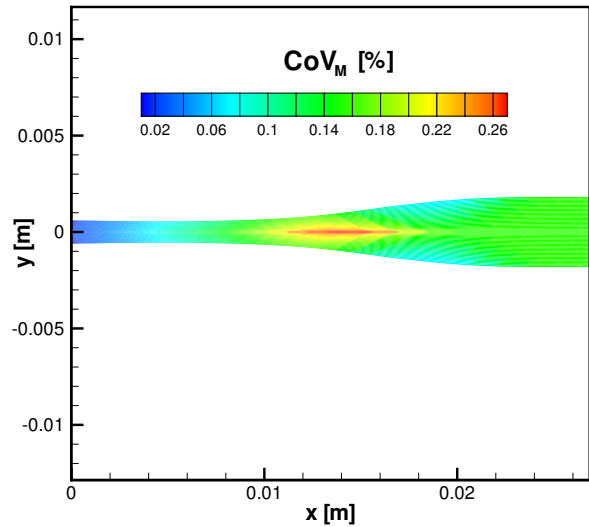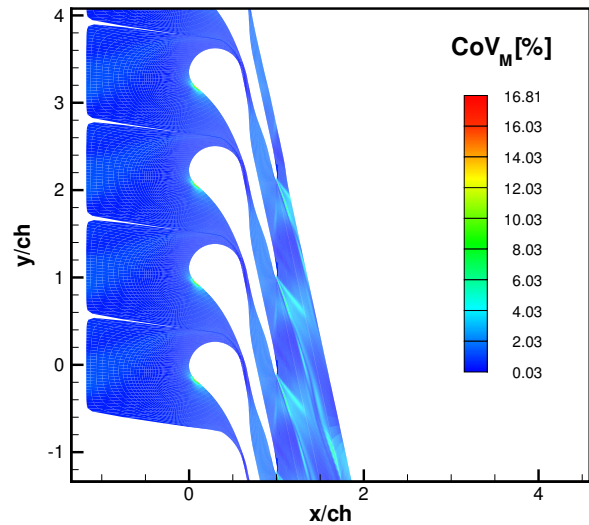
## Sensitivity analysis via ANOVA

Here a ANOVA decomposition analysis is proposed. The procedure is applied at the Mach number variance evo-
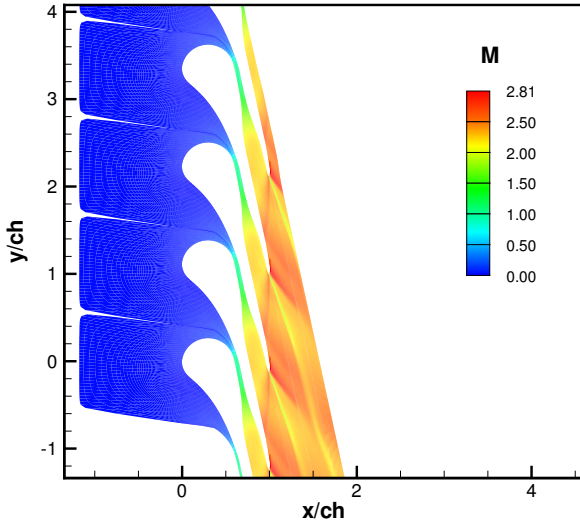
**FIGURE 17**. MEAN MACH NUMBER CONTOUR PLOT FOR BETA DISTRIBUTED INPUT PARAMETERS (8% COEFFICIENT OF VARIATION) FOR AN INVISCID STOCHASTIC CALCULATION.

lution and implements the evaluation of the Sobol' indices for each source of uncertainty [26] and aims to identify the main contributors to the total variance estimated with the full-factorial PCM algorithm. Even though the PCM represents a numerically expensive method, it is very accurate [27] and is here implemented for obtaining a reference solution. Comparisons with other more efficient uncertainty quantification methods are in progress and will be discussed in the future.

In this problem five uncertain input parameters are taken into account: two operating conditions $(p_r^0, T_r^0)$ and three geometric factors (angle of attach $\beta_a$, blade stagger angle $\theta$ and blade thickness $\epsilon$). In this set the thermodynamic parameters have been neglected in order to reduce the space parameters and save computational cost. Indeed, as shown by other authors [27], the thermodynamic model plays a marginal role in this kind of application. In this way, by considering a second order Lagrange interpolated chaos polynomial, the total number of collocation points (and, then, of deterministic simulations) is $P_{PCM} = 3^5 = 243$. The results are obtained in the same hypotheses of the two-parameter calculations: uniformly distributed input parameters; operating conditions variability of 3% respect to the nominal point ($p_r^0 = 0.98, T_r^0 = 1.13$). It has been imposed a variability of 1% around the base injector shape for the geometric parameters. These values agree with the common geomet-

ric tolerances for turbomachinery applications.

In Fig. 19 the mean Mach number field is shown. It is qualitatively similar to those previously obtained with other simulations and no further considerations will be carried out. More significant informations are provided by Fig. 18, where the Mach number percent coefficient of variation is shown. The amplification factor given by the exit-to-inlet $CoV_M$ ratio, evaluated for the Mach number, is about 0.667. This value states the existence of a damping effect of the upstream uncertainties provided by the injector system. Besides, even though the level of uncertainty for the operational input parameters is the same of the uniform two-parameter case, the variability of the output reaches higher level which are comparable with those obtained with the Beta distribution calculation. This result could be explained by asserting that the introduction of , and most of all, variations of the pressure ratio have increased the global level of uncertainty. To verify this claim the ANOVA analysis can helps to evaluate the contribution of the single uncertain parameters to the global variance.

Here only first order Sobol' indices are evaluated and the second order parameter interactions are neglected. In Fig. 20 the five Sobol' indices are shown. It is clear that the operating conditions $(p_r^0, T_r^0)$, with greatest importance of the inlet total pressure, and the geometric parameters $(\beta_a, \epsilon)$ give a great contribution to the final value of the Mach number variance. On the contrary, the stagger angle $\theta$ seems to have a negligible action. In Fig. 21 the percent contribution to the variability of the nozzle blade performances by means of isentropic efficiency and power output, for each input parameter, is shown. The histogram confirms the importance of the operating conditions on the final results, along with minor contributions given by the blade thickness and the angle of attach.

## CONCLUSIONS

In this work a fast methodology design for supersonic nozzle blade vanes of ORC axial turbines has been developed and tested for accuracy analysis. The design process, based on the method of characteristics (MOC), takes into account the complex behaviour of the ORC working fluids, characterised by strong dense gas effects under the operating conditions of interest. The MOC is generalized to the real gas case and accurate multiparameter equations of state are used to model the gas thermodynamic behaviour. Then, numerical simulations are carried out for the blade vane design at nominal operating conditions near to the critical point for the ORC suitable R245fa working fluid. It is shown that there is the presence of dense gas effects which have an impact on the injector performances. Indeed, by analysing the fundamental derivative behaviour, the shock
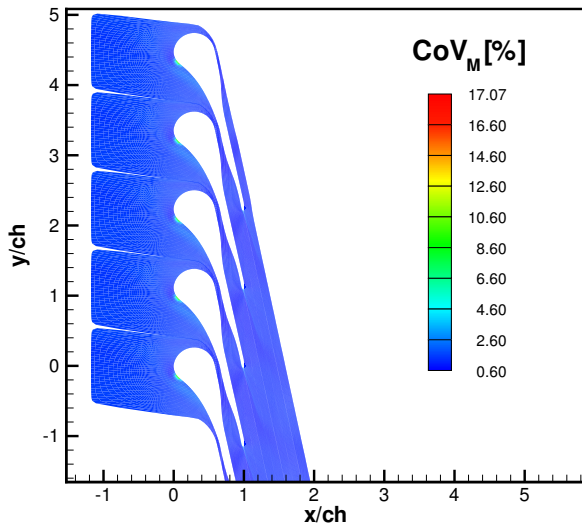
**FIGURE 18**. COEFFICIENT OF VARIATION OF MACH NUMBER FOR FIVE UNIFORMLY DISTRIBUTED INPUT PARAMETERS FOR AN INVISCID STOCHASTIC CALCULATION.
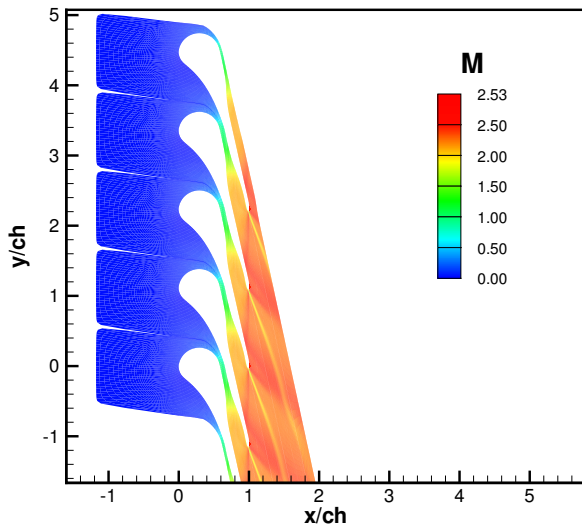


**FIGURE 19**. MEAN MACH NUMBER CONTOUR PLOT FOR FIVE UNIFORMLY DISTRIBUTED INPUT PARAMETERS FOR AN INVISCID STOCHASTIC CALCULATION.

intensity is lower than in the ideal gas case and this effect has positive consequences on the main performances.
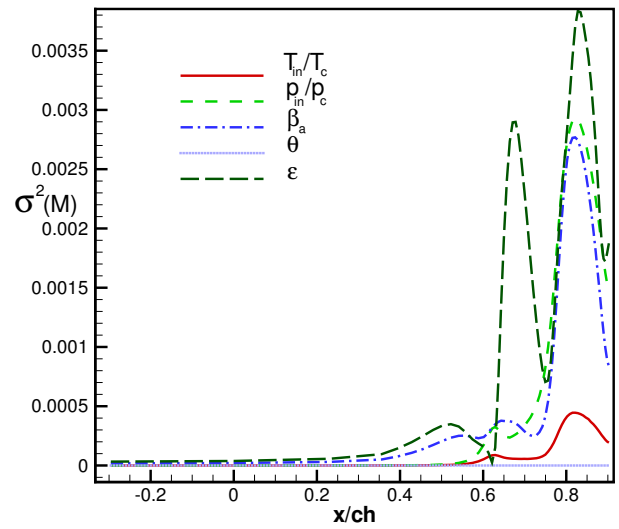


**FIGURE 20**. ANOVA OF THE CONTRIBUTION OF THE FIVE INPUT PARAMETERS TO THE VARIANCE OF MACH NUMBER. VALUES EVALUATED ALONG THE BLADE VANE AXIS.
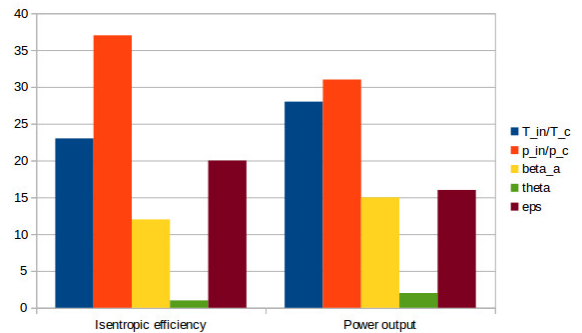


**FIGURE 21**. PERCENT FIRST ORDER CONTRIBUTION OF EACH UNCERTAINTY TO THE NOZZLE BLADE PERFORMANCES.

An uncertainty quantification analysis is then carried out by studying the sensitivity of the MOC algorithm to the variability of the operating conditions. It has been shown that the MOC method is quite robust to variations of the magnitude of 8% , for a given mass flow ratio.. Further tests could be performed by increasing even more the input variability and changing the target massflow rate in order to variate the exit-to-throat nozzle area ratio and assess the limits of the MOC robustness.

In the last part of the paper a ANOVA decomposition anal-

ysis is carried out to identify the greatest contributions to the variance of the Mach number and, ultimately, of the injector performances such as isentropic efficiency and power output. The results show a great influence of the operational parameters and of two geometrical ones, as the blade thickness and the angle of attach, on the output performances.

## REFERENCES

[1] Maizza, V., and Maizza, A., 2001. "Unconventional working fluids in organic rankine-cycles for waste energy recovery systems". *Applied Thermal Engineering,* *21*(3), pp. 381–390.

[2] Hung, T., Shai, T., and Wang, S., 1997. "A review of organic rankine cycles (orcs) for the recovery of low-grade waste heat". *Energy,* *22*(7), pp. 661–667.

[3] Cinnella, P., and Hercus, S., 2010. "Robust optimization of dense gas flows under uncertain operating conditions". *Computers & Fluids,* *39*(10), pp. 1893–1908.

[4] Hercus, S. J., and Cinnella, P., 2011. "Robust shape optimization of uncertain dense gas flows through a plane turbine cascade". In ASME-JSME-KSME 2011 Joint Fluids Engineering Conference, American Society of Mechanical Engineers, pp. 1739–1749.

[5] Zucrow, M. J., and Hoffman, J. D., 1976. "Gas dynamics". *New York: Wiley, 1976,* *1–2*.

[6] Délery, J., 2010. *Handbook of compressible aerodynamics.* ISTE.

[7] Ali, M., Mashud, M., Al Bari, A., and Islam, M. M.-U., 2006. "Numerical solution for the design of minimum length supersonic nozzle.".

[8] van der Waals, J. D., 1913. "The law of corresponding states for different substances". In KNAW, Proceedings, Vol. 15, pp. 1912–1913.

[9] Thompson, P. A., 1971. "A fundamental derivative in gasdynamics". *Physics of Fluids (1958-1988),* *14*(9), pp. 1843–1849.

[10] Bethe, H., 1998. "On the theory of shock waves for an arbitrary equation of state". In *Classic Papers in Shock Compression Science*. Springer, pp. 421–495.

[11] Cramer, M., and Tarkenton, G., 1992. "Transonic flows of bethe-zel'dovich-thompson fluids". *Journal of Fluid Mechanics,* *240*, pp. 197–228.

[12] Cinnella, P., and Congedo, P. M., 2007. "Inviscid and viscous aerodynamics of dense gases". *Journal of Fluid Mechanics,* *580*, pp. 179–217.

[13] Stryjek, R., and Vera, J., 1986. "Prsv: An improved peng-robinson equation of state for pure compounds and mixtures". *The canadian journal of chemical engineering,* *64*(2), pp. 323–333.

[14] Congedo, P., Corre, C., and Martinez, J.-M., 2011. "Shape optimization of an airfoil in a BZT flow with multiple-source uncertainties". pp. 216 – 232.

[15] Colonna, P., Nannan, N., Guardone, A., and Lemmon, E., 2006. "Multiparameter equations of state for selected siloxanes". pp. 193 – 211.

[16] Colonna, P., Guardone, A., and Nannan, N., 2007. "Siloxanes: A new class of candidate Bethe-Zel'dovich-Thompson fluids".

[17] Colonna, P., Nannan, N., and Guardone, A., 2008. "Multiparameter equations of state for siloxanes: $[(CH_3)_3\text{-}Si\text{-}O_{1/2}]_2\text{-}[O\text{-}Si\text{-}(CH_3)_2]_{i=1,...,3}$, and $[O\text{-}Si\text{-}(CH_3)_2]_6$". pp. 115 – 130.

[18] Cinnella, P., and Congedo, P. M., 2005. "Numerical solver for dense gas flows". *AIAA journal,* *43*(11), pp. 2458–2461.

[19] Jameson, A., Schmidt, W., Turkel, E., et al., 1981. "Numerical solutions of the euler equations by finite volume methods using runge-kutta time-stepping schemes". *AIAA paper,* *1259*, p. 1981.

[20] Rezgui, A., Cinnella, P., and Lerat, A., 2001. "Third-order accurate finite volume schemes for euler computations on curvilinear meshes". *Computers & fluids,* *30*(7), pp. 875–901.

[21] Cinnella, P., and Congedo, P. M., 2005. "Aerodynamic performance of transonic bethe-zal'dovich-thompson flows past an airfoil". *AIAA journal,* *43*(2), pp. 370–378.

[22] Carriere, P., 1972. *Dynamique des gaz, vol. 1–2.* ENSTA.

[23] Lemmon, E. W., Huber, M. L., and McLinden, M. O., 2013. *NIST Reference Fluid Thermodynamic and Transport Properties - REFPROP Version 9.1.* NIST.

[24] Loeven, A., Witteveen, J., and Bijl, H., 2007. "Probabilistic collocation: An efficient non-intrusive approach for arbitrarily distributed parametric uncertainties". In 45th AIAA Aerospace Sciences Meeting and Exhibit, no. AAIA Paper 2007-317.

[25] Xiu, D., and Karniadakis, G., 2003. "Modeling uncertainty in flow simulations via generalized polynomial chaos". pp. 137–167.

[26] TANG, G., Eldred, M., and SWILER, L. P., 2010. "Global sensitivity analysis for stochastic collocation expansion". *CSRI Summer Proceedings,* *2009*, p. 100.

[27] Congedo, P. M., Cinnella, P., Hercus, S., Corre, C. E., et al., 2011. "Efficient robust optimization techniques for uncertain dense gas flows". In CFD & Optimization-ECCOMAS Thematic Conference.